The ATLAS Trigger – Commissioning with cosmic rays

Abolins M.[44], Achenbach R.[25], Adragna P.[61], Aielli G.[66], Aleksandrov E.[18], Aleksandrov I.[18], Aloisio A.[55], Alviggi M.G.[55], Amorim A.[38], Anderson K.[14], Andrei V.[25], Anduaga X.[39], Antonelli S.[9], Aracena I.[67], Ask S.[12], Asquith L.[78], Avolio G.[12], Backlund S.[12], Badescu E.[10], Bahat Treidel O.[73], Baines J.[62], Barnett B.M.[62], Barria P.[65,31], Bartoldus R.[67], Batreanu S.[10,12], Bauss B.[45], Beck H.P.[6], Bee C.[48], Bell P.[46], Bell W.H.[22], Bellagamba L.[9], Bellomo M.[60], Ben Ami S.[73], Bendel M.[45], Benhammou Y.[74], Benslama K.[63], Berge D.[12], Berger N.[36,29], Berry T.[27], Bianco M.[41], Biglietti M.[55], Blair R. R.[1], Bogaerts A.[12], Bohm C.[72], Bold T.[77], Booth J.R.A.[7,62], Boscherini D.[9], Bosman M.[5], Boyd J.[12], Brawn I.P.[62], Brelier B.[50], Bressler S.[73], Bruni A.[9], Bruni G.[9], Buda S.[10], Burckhart-Chromek D.[12], Buttar C.[22], Camarri P.[66], Campanelli M.[44], Canale V.[55], Caprini M.[10], Caracinha D.[42], Cardarelli R.[66], Carlino G.[55], Casadei D.[53], Casado P.[5], Cataldi G.[41], Cerri A.[12], Charlton D.G.[7], Chiodini G.[41], Ciapetti G.[65,31], Cimino D.[30], Ciobotaru M.[10,77,12], Clements D.[22], Coccaro A.[21], Coluccia M.R.[41], Conde Muino P.[38], Constantin S.[10], Conventi F.[55], Corso-Radu A.[77], Costa M.J.[79], Coura Torres R.[64], Cranfield R.[78], Cranmer K.[53], Crone G.[78], Curtis C.J.[7], Dam M.[52], Damazio D.[4], Davis A.O.[62], Dawson I.[70], Dawson J.[1], De Almeida Simoes J.[42], De Cecco S.[65,31], De Pedis D.[65,31], De Santo A.[27], DeAsmundis R.[55], DellaPietra M.[55], DellaVolpe D.[55], Delsart P.-A.[50], Demers S.[67], Demirkoz B.[12], Di Mattia A.[44], DiCiaccio A.[66], DiGirolamo A.[65,31], Dionisi C.[65,31], Djilkibaev R.[53], Dobinson R.[12], Dobson M.[12], Dogaru M.[10], Dotti A.[30], Dova M.[39], Drake G.[1], Dufour M.-A.[49], Eckweiler S.[45], Ehrenfeld W.[16], Eifert T.[20], Eisenhandler E.[61], Ellis N.[12], Emeliyanov D.[62], Enoque Ferreira de Lima D.[64], Ermoline Y.[44], Eschrich I.[77], Etzion E.[74], Facius K.[52], Falciano S.[31], Farthouat P.[12], Faulkner P.J.W.F.[7], Feng E.[14], Ferland J.[50], Ferrari R.[60], Ferrer M.L.[19], Fischer G.[28], Fonseca-Martin T.[12], Francis D.[12], Fukunaga C.[76], Fohlisch F.[25], Gadomski S.[6], Garitaonandia Elejabarrieta H.[5], Gaudio G.[60], Gaumer O.[20], Gee C.N.P.[62], George S.[27], Geweniger C.[25], Giagu S.[65,31], Gillman A.R.[62], Giusti P.[9], Goncalo R.[27], Gorini B.[12], Gorini E.[69,41], Gowdy S.[67], Grabowska-Bold I.[12], Grancagnolo F.[41], Grancagnolo S.[69,41], Green B.[27], Galllno P.[12], Haas S.[12], Haberichter W.[1], Hadavand H.[68], Haeberli C.[6], Haller J.[24,16], Hamilton A.[20], Hanke P.[25], Hansen J.R.[52], Hasegawa Y.[71], Hauschild M.[12], Hauser R.[44], Head S.[46], Hellman S.[72], Hidvegi A.[72], Hillier S.[7],

Hoecker A.[12], Hryn'ova T.[12], Hughes-Jones R.[46], Huston J.[44], Iacobucci G.[9], Idarraga J.[50], Iengo P.[55], Igonkina O.[57], Ikeno M.[34], Inada M.[35], Ishino M.[75], Iwasaki H.[34], Izzo V.[55], Jain V.[32], Johansen M.[72], Johns K.[3], Joos M.[12], Kadosaka T.[35], Kajomovitz E.[73], Kama S.[16], Kanaya N.[35], Kawagoe K.[35], Kawamoto T.[75], Kazarov A.[59], Kehoe R.[68], Khoriauli G.[63], Kieft G.[56], Kilvington G.[27], Kirk J.[62], Kiyamura H.[35], Klofver P.[12], Klous, S.[56], Kluge E.-E.[25], Kobayashi T.[75], Kolos S.[77], Kono T.[12], Konstantinidis N.[78], Korcyl K.[15], Kordas K.[6], Kotov V.[18], Krasznahorkay A.[12,17], Kubota T.[75], Kugel A.[47], Kuhn D.[33], Kurashige H.[35], Kurasige H.[35], Kuwabara T.[75], Kwee R.[83], Landon M.[61], Lankford A.[77], LeCompte T.[1], Leahu L.[10,12], Leahu M.[10], Ledroit F.[23], Lehmann Miotto G.[12], Lei X.[3], Lellouch D.[81], Lendermann V.[25], Levinson L.[81], Leyton M.[37], Li S.[16], Liberti B.[66], Lifshitz R.[73], Lim H.[1], Lohse T.[28], Losada M.[8], Luci C.[65,31], Luminari L.[31], Lupu N.[73], Mahboubi K.[25], Mahout G.[7], Mapelli L.[12], Marchese F.[66], Martin B.[12], Martin B.T.[44], Martinez A.[79], Marzano F.[31], Masik J.[46], McMahon T.[27], Mcpherson R.[80], Medinnis M.[16], Meessen C.[48], Meier K.[25], Meirosu C.[10], Messina A.[12], Migliaccio A.[55], Mikenberg G.[81], Mincer A.[53], Mineev M.[18], Misiejuk A.[27], Moenig K.[83], Monticelli F.[39], Moraes A.[4], Moreno D.[8], Morettini P.[21], Murillo Garcia R.[12], Nagano K.[34], Nagasaka Y.[26], Negri A.[77], Nemethy P.[53], Neusiedl A.[45], Nisati A.[65,31], Niwa T.[35], Nomachi M.[58], Nomoto H.[75], Nozaki M.[34], Nozicka M.[16], Ochi A.[35], Ohm C.[12], Okumura Y.[54], Omachi C.[35], Osculati B.[21], Oshita H.[71], Osuna C.[5], Padilla C.[12], Panikashvili N.[73], Parodi F.[21], Pasqualucci E.[65,31], Pastore F.[65,31], Patricelli S.[55], Pauly T.[12], Pectu M.[10], Perantoni M.[64], Perera V.[62], Perera V.J.O.[62], Perez E.[5], Perez Reale V.[12], Perrino R.[41], Pessoa Lima Junior H.[64], Petersen J.[12], Petrolo E.[65,31], Piegaia R.[11], Pilcher J.[14], Pinto F.[11], Pinzon G.[8], Polini A.[9], Pope B.[44], Potter C.[49], Prieur D.P.F.[62], Primavera M.[41], Qian W.[62], Radescu V.[16], Rajagopalan S.[4], Renkel P.[68], Rescigno M.[65], Rieke S.[45], Risler C.[28], Riu I.[5], Robertson S.[49], Roda C.[30], Rodriguez D.[8], Rogriquez Y.[8], Roich A.[81], Romeo G.[11], Rosati S.[65,31], Ryabov Y.[59], Ryan P.[44], Rhr F.[25], Sakamoto H.[75], Salamon A.[66], Salvatore D.[13], Sankey D.P.C.[62], Santamarina C.[49], Santamarina Rios C.[49], Santonico R.[66], Sasaki O.[34], Scannicchio D.[60], Scannicchio D.A.[60], Schiavi C.[21], Schlereth J.[1], Schmitt K.[25], Scholtes I.[12], Schooltz D.[44], Schuler G.[12], Schultz-Coulon H.-C.[25], Schfer U.[45], Scott W.[62], Segura E.[5], Sekhniaidze G.[55], Shimbo N.[35], Sidoti A.[31], Silva L.[11], Silverstein S.[72], Siragusa G.[69,41], Sivoklokov S.[51], Sloper J.E.[12], Smizanska M.[40], Solfaroli E.[66], Soloviev I.[12], Soluk R.[2], Spagnolo S.[69,41], Spila F.[65,31], Spiwoks R.[12], Staley R.J.[7], Stamen R.[25], Stancu S.[10,77,12], Steinberg P.[4], Stelzer J.[12], Stradling A.[82], Strom D.[57], Strong J.[27], Su D.[67], Sugaya Y.[58], Sugimoto T.[54], Sushkov S.[5], Sutton M.[78], Szymocha T.[15], Takahashi Y.[54], Takeda H.[35], Takeshita T.[71], Tanaka S.[34], Tapprogge S.[45], Tarem S.[73], Tarem Z.[73], Teixeira-Dias P.[27], Thomas J.P.[7], Tokoshuku K.[34], Tomoto M.[54], Torrence E.[57], Touchard F.[48], Trefzger T.[45], Tremblet L.[12], Tripiana M.[39], Usai G.[14], Vachon B.[49], Vandelli W.[12], Vari R.[65,31], Veneziano S.[65,31], Ventura A.[41], Vercesi V.[60], Vermeulen J.[56], Von Der Schmitt J.[43], Wang M.[63], Watkins P.M.[7], Watson A.[7], Weber P.[25], Wengler

T.[46], Werner P.[12], Wheeler-Ellis S.[77], Wickens F.[62], Wiedenmann W.[82], Wielers M.[62], Wilkens H.[12], Winklmeier F.[12], Woehrling E.-E.[7], Wu S.-L.[82], Wu X.[20], Xella S.[52], Yamaguchi Y.[75], Yamazaki Y.[34], Yasu Y.[34], Yu M.[47], Zanello L.[65,31], Zema F.[12], Zhang J.[1], Zhao L.[53], Zobernig H.[82], de Seixas J.M.[64], dos Anjos A.[82], zur Nedden M.[28], Ozcan E.[78] and Unel G.[77,12]

1 Argonne National Laboratory, Argonne, Illinois
2 University of Alberta, Edmonton
3 University of Arizona, Tucson, Arizona
4 Brookhaven National Laboratory (BNL), Upton, New York
5 Institut de Fsica d'Altes Energies (IFAE), Universitat Autnoma de Barcelona, Bellaterra (Barcelona)
6 Laboratory for High Energy Physics, University of Bern, Bern
7 School of Physics and Astronomy, The University of Birmingham, Birmingham
8 Universidad Antonio Narino, Bogot, Colmbia
9 Dipartimento di Fisica dell' Universit di Bologna e I.N.F.N., Bologna
10 National Institute for Physics and Nuclear Engineering, Institute of Atomic Physics, Bucharest
11 Univerity of Buenos Aires, Buenos Aires
12 European Laboratory for Particle Physics (CERN), Geneva
13 Dipartimento di Fisica dell' Universit della Calabria e I.N.F.N., Cosenza
14 University of Chicago, Enrico Fermi Institute, Chicago, Illinois
15 Institute of Nuclear Physics, Polish Academy of Sciences, Cracow
16 Deutsches Elektronen-Synchrotron (DESY), Hamburg
17 University of Debrecen
18 Joint Institute for Nuclear Research, Dubna
19 Laboratori Nazionali di Frascati dell' I.N.F.N., Frascati
20 Section de Physique, Universit de Genve, Geneva
21 Dipartimento di Fisica dell' Universit di Genova e I.N.F.N., Genova
22 Department of Physics and Astronomy, University of Glasgow, Glasgow
23 Laboratoire de Physique Subatomique et de Cosmologie de Grenoble (LPSC), IN2P3-CNRS-Universit Joseph Fourier, Grenoble
24 University of Hamburg, Germany
25 Kirchhoff Institut fr Physik, Heidelberg
26 Hiroshima Institute of Technology, Hiroshima
27 Department of Physics, Royal Holloway and Bedford New College, Egham
28 Institut fr Physik, Humboldt Universitt, Berlin
29 Institut National de Physique Nucleaire et de Physique des Particules
30 Dipartimento di Fisica dell' Universit di Pisa e I.N.F.N., Pisa
31 I.N.F.N. Roma
32 Indiana University, Bloomington, Indiana
33 Institut fr Experimentalphysik der Leopold-Franzens-Universitt Innsbruck, Innsbruck
34 KEK, High Energy Accelerator Research Organisation, Tsukuba
35 Kobe University, Kobe
36 Laboratoire d'Annecy-le-Vieux de Physique des Particules (LAPP), IN2P3-CNRS, Annecy-le-Vieux
37 Lawrence Berkeley Laboratory and University of California, Berkeley, California
38 Laboratorio de Instrumentacao e Fisica Experimental, Lisboa
39 National University of La Plata, La Plata
40 Department of Physics, Lancaster University, Lancaster
41 Dipartimento di Fisica dell' Universit di Lecce e I.N.F.N., Lecce
42 University Catlica-Figueira da Foz and University Nova de Lisboa, Lisbon
43 Max-Planck-Institut fr Physik, Mnchen
44 Michigan State University, Department of Physics and Astronomy, East Lansing, Michigan
45 Institut fr Physik, Universitt Mainz, Mainz
46 Department of Physics and Astronomy, University of Manchester, Manchester
47 Lehrstuhl fr Informatik V, Universitt Mannheim, Mannheim
48 Centre de Physique des Particules de Marseille, IN2P3-CNRS, Marseille

49 Department of Physics, McGill University, Montreal
50 University of Montreal, Montreal
51 Moscow State University, Moscow
52 Niels Bohr Institute, University of Copenhagen, Copenhagen
53 Department of Physics, New York University, New York
54 Nagoya University, Nagoya
55 Dipartimento di Scienze Fisiche, Universit di Napoli 'Federico II' e I.N.F.N., Napoli
56 FOM - Institute SAF NIKHEF and University of Amsterdam/NIKHEF, Amsterdam
57 University of Oregon, Eugene, Oregon
58 Osaka University, Osaka
59 Petersburg Nuclear Physics Institute (PNPI), St. Petersburg
60 Dipartimento di Fisica Nucleare e Teorica dell' Universit di Pavia e I.N.F.N., Pavia
61 Department of Physics, Queen Mary and Westfield College, University of London, London
62 Rutherford Appleton Laboratory, Chilton, Didcot
63 University of Regina, Regina
64 Universidade Federal do Rio de Janeiro, COPPE/EE/IF, Rio de Janeiro
65 Dipartimento di Fisica dell' Universit di Roma I 'La Sapienza'
66 Dipartimento di Fisica dell' Universit di Roma II 'Tor Vergata'
67 Stanford Linear Accelerator Center (SLAC), Stanford
68 Department of Physics, Southern Methodist University, Dallas, Texas
69 Universit degli Studi del Salento
70 Department of Physics, University of Sheffield, Sheffield
71 Faculty of Science, Shinshu University, Matsumoto
72 Stockholm University, Stockholm
73 Department of Physics, Technion, Haifa
74 School of Physics, Tel-Aviv University, Tel-Aviv
75 International Center for Elementary Particle Physics, University of Tokyo, Tokyo
76 Physics Department, Tokyo Metropolitan University, Tokyo
77 University of California, Irvine, California
78 Department of Physics and Astronomy, University College London, London
79 Instituto de Fisica Corpuscular (IFIC) Universidad de Valencia
80 University of Victoria, Victoria
81 Department of Particle Physics, The Weizmann Institute of Science, Rehovot
82 Department of Physics, University of Wisconsin, Madison, Wisconsin
83 Deutsches Elektronen-Synchrotron (DESY), Zeuthen

Abstract.   The ATLAS detector at CERN's LHC will be exposed to proton-proton collisions from beams crossing at 40 MHz. At the design luminosity there are roughly 23 collisions per bunch crossing. ATLAS has designed a three-level trigger system to select potentially interesting events. The first-level trigger, implemented in custom-built electronics, reduces the incoming rate to less than 100 kHz with a total latency of less than 2.5μs. The next two trigger levels run in software on commercial PC farms. They reduce the output rate to 100-200 Hz.

In preparation for collision data-taking which is scheduled to commence in May 2008, several cosmic-ray commissioning runs have been performed. Among the first sub-detectors available for commissioning runs are parts of the barrel muon detector including the RPC detectors that are used in the first-level trigger. Data have been taken with a full slice of the muon trigger and readout chain, from the detectors in one sector of the RPC system, to the second-level trigger algorithms and the data-acquisition system. The system is being prepared to include the inner-tracking detector in the readout and second-level trigger.

We will present the status and results of these cosmic-ray based commissioning activities. This work will prove to be invaluable not only during the commissioning phase but also for cosmic-ray data-taking during the normal running for detector performance studies.
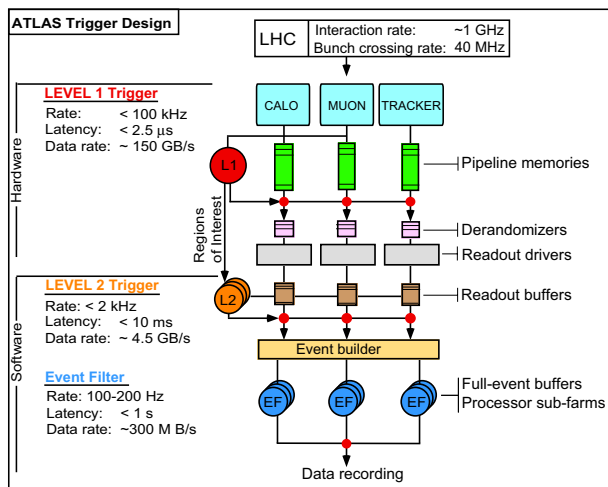
Figure 1. The layout of the trigger system of ATLAS is shown here. There are three selection levels. The first one is in hardware, the second and third ones are done in software. In the level-1, the trigger decision is based on coarse-resolution input from muon trigger and calorimeter detectors, the data of the inner detector is only used in the higher trigger levels. The algorithms of the level-2 make use of only a fraction of the high-resolution event data, guided by regions of interest data received from the level-1 trigger. The level-3 trigger algorithms refine the trigger decision once more based on the full event information.

1. Introduction

The event selection at the LHC is a very challenging task. At the design luminosity of 10^{34} cm^{-2} s^{-1} there are on average 23 collisions per bunch crossing. With beams crossing at 40 MHz, this gives an interaction rate of 1 GHz. The rate is dominated by the inelastic part of the total cross-section, which is about 70 mb. The cross-sections of many of the interesting physics processes are a factor of 10^6 below that value. For example, at design luminosity the cross-section for inclusive W production leads to a rate of 1400 Hz, whereas the rates for some rare physics processes are much smaller. For the Standard Model Higgs boson for example with a mass of 150 GeV the rate is expected to be in the sub-Hz region. Thus a powerful selection is needed to extract the interesting physics signals from the vast background.

The full event size of ATLAS is on the order of 1.5 MB. With 40 MHz incoming rate, this would result in a data rate of 60 TB/s, way beyond current network and storage capabilities. Hence an online selection, that is, a trigger system, has to be set in place to reduce the incoming rate to an affordable level of 100-200 Hz (aiming at a data rate of $\sim$ 300 MB/s) while retaining potentially interesting physics events.

ATLAS has designed a three-level trigger system which has the demanding task of finding the five in one million events that can be recorded. It aims at selecting with the greatest possible efficiency and least possible bias the interesting physics events and is largely based on signatures of high-transverse-momentum particles and large missing transverse energy.

The sketch in Fig. 1 gives an overview of the design of the trigger system of ATLAS. The trigger is split in three steps. The first level (LVL1) [1] is based on coarse-resolution data from the calorimeters and dedicated fast muon detectors. It consists of the calorimeter trigger, the muon trigger, and the central trigger system. The output rate of LVL1 is required to be less than 100 kHz with an allowed latency of 2.5 μs. The corresponding output data rate amounts to $\sim$ 150 GB/s. The remaining two trigger levels, the level-2 trigger (LVL2) and the event filter, are implemented in software and run on commercial PC farms [2]. The LVL2 trigger
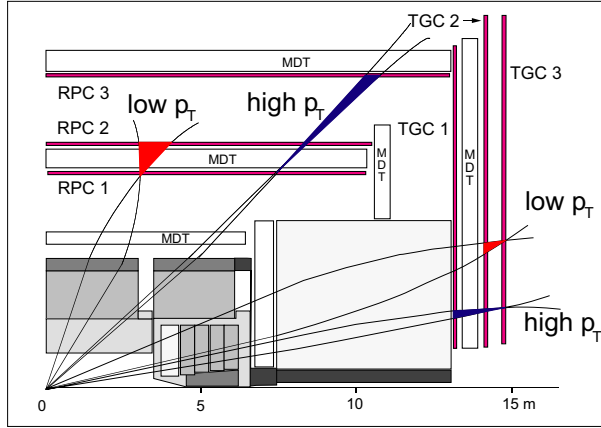
Figure 2. Schema of the level-1 muon barrel trigger. The trigger is based on three stations. The two low-p_T inner stations, RPC1 and RPC2, are arranged on either side of the middle station of the precision chambers (MDT), at 7.8 m and 8.3 m from the interaction point. The high-p_T station RPC3 is just inside the outer MDT station at 10.2 m radial distance.

design is a unique feature of ATLAS. It is based on the concept of "regions of interests" (RoIs). Algorithms request full-resolution data only from a fraction of the detector, from regions that were identified by the LVL1 trigger as *regions of interest*. For that purpose, event information like the coordinates of a particle candidate or energy and momentum values are generated by the LVL1 trigger systems and sent to the LVL2 trigger processors. Thereby the amount of full-resolution data that is accessed by the LVL2 is less than 10% of the total event size significantly reducing the processing time[1]. At LVL2 the rate is reduced by about a factor of 50 to a few kHz with an allowed latency of 10 ms. The event filter in turn has access to the full resolution data of the whole detector; it processes fully assembled events. It runs offline-like reconstruction and selection algorithms and has to provide another factor of 10 in rate reduction within a processing time of ~ 1 s to arrive at the final storage rate of 100-200 Hz.

2. The ATLAS LVL1 Trigger System
The first-level trigger system of ATLAS synchronously processes information from the calorimeter and muon trigger detectors at the heartbeat of the LHC, the proton-proton bunch-crossing frequency of 40.08 MHz. It comprises three sub-systems, the calorimeter trigger, the muon trigger, and the central-trigger system.

For cosmic ray commissioning the most important LVL1 trigger is the muon barrel trigger.

2.1. The LVL1 Muon Barrel Trigger
The ATLAS muon spectrometer consists of monitored drift tube (MDT) muon chambers for precision measurements and dedicated fast muon detectors for providing information about muon candidates to the LVL1 Central Trigger. The trigger chambers are resistive-plate chambers (RPCs) in the barrel region ($|\eta| < 1.05$) and thin-gap chambers (TGCs) for the end-caps ($1.05 < |\eta| < 2.4$). The trigger selects muon candidates based on transverse momentum (p_T). The trigger detectors in both the barrel and the end-caps are sub-divided in η and ϕ space into trigger sectors. In total there are 64 sectors for the barrel and 144 sectors for the end-caps. Each sector is sub-divided into RoIs with typical sizes of approximately $\Delta\eta \times \Delta\phi = 0.1 \times 0.1$.

---

[1] In fact for most events the amount of data that is accessed by the LVL2 algorithms will be even on the order of 2%.
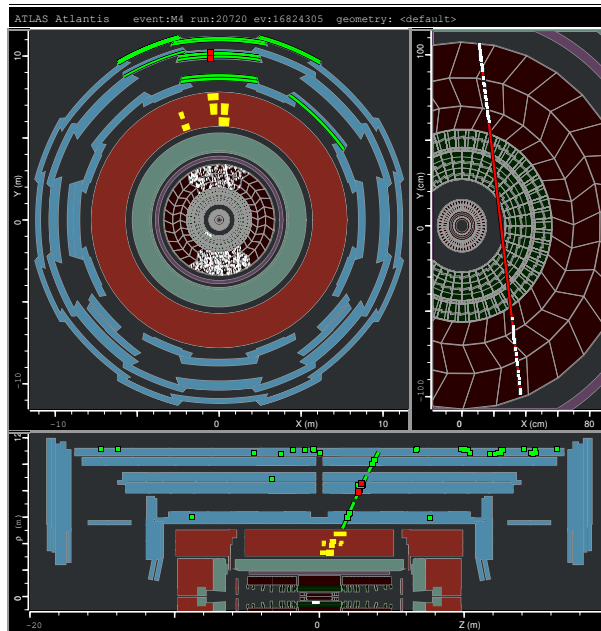
Figure 3. An event display picture of an event taken in the August combined run. This event shows hits in the RPC and MDT muon stations as well as hits in the Tile calorimeter and the TRT (inset on right). The top plots show an x-y view of the detector whereas the bottom shows an z-y view.

For further descriptions of the LVL1 muon trigger system, see [1].

3. Cosmic ray commissioning

In June and August 2007 two, ten day combined cosmic ray runs were taken with much of the ATLAS detector used. The runs involved the following systems:

- Muons (RPC, MDT and TGC)
- Calorimeters (LAr electromagnetic calorimeter and Tile hadronic calorimeter)
- Transisition Radiation Tracker (TRT)

All systems had partial coverage ranging from $\frac{1}{64}$ to $\approx \frac{1}{2}$ of the system. The only systems missing were the muon Cathode Strip Chambers and the silicon strip and pixel detectors. Figure 3 shows an event display picture of an event taken in the August combined run. This event shows hits in the RPC and MDT muon stations as well as hits in the Tile calorimeter and the TRT.

3.1. The LVL1 setup

For both of the combined cosmic runs the LVL1 trigger was provided by the barrel and endcap muon triggers as well as a trigger from the Tile calorimeter that was implemented temporarily for the cosmic ray running. The LVL1 calorimeter trigger was being commissioned during the August run, but was not providing triggers.

In the June run half of one RPC sector was used for the LVL1 ($\frac{1}{32}$ of the barrel) and 1 sector of one side of the TGC endcap. In August the RPC coverage was increased to 1 sector ($\frac{1}{16}$), while the TGC coverage was the same.

The rate observed from the RPC trigger was $\approx 100\,\text{Hz}$ which was consistent with expectations from simulation. The rate from the TGC was $\approx 1\,\text{Hz}$ and for the trigger from the Tile calorimeter

was ≈ 0.1 Hz. Despite the low rate the Tile trigger is useful for obtaining events that are likely to have TRT tracks in them as the Calorimeters are much closer to the TRT barrel than the muon system.

3.2. HLT algorithms for commissioning

The HLT was run online for the first time in the summer 2007 cosmic runs. The algorithms run were either designed specifically for cosmic rays or modified from physics algorithms. Running these algorithms proves very useful for testing many stages of the full trigger chain. Some of the most important aspects of the trigger that are tested are:

- The interface from the muon systems to the LVL1
- Distribution of LVL1 trigger and timing signal (LVL1 Accept, clock and the busy signal)
- The input data to LVL2 using the RoI mechanism
- The configuration of the HLT [3]
- The steering of the HLT [4]

The hardware on which the HLT was run during the summer 2007 was a subset ($\approx 4\%$) of the final hardware to be used during ATLAS dataking. More details on the hardware can be seen in [5].

All the algorithms run during the summer 2007 cosmic runs were tested on simulated cosmic ray samples. More details on the cosmic simulation can be seen at [6]. The algorithms were all run in forced accept mode so no event rejection was carried out.

3.3. Algorithms run in June cosmic run

For the June cosmic run two LVL2 algorithms were run online. One was a dedicated algorithm for finding cosmic rays using the muon systems (RPC and MDT), and the other used the LAr calorimeter.

The muon algorithm uses RPC hits in the middle RPC station as a seed and then combines RPC hits in the inner or outer stations to form a straight line RPC track. MDT hits are then searched for in the MDT stations aound the RPC track and then MDT track segments are formed from these MDT hits in each of the 3 MDT stations. Finally the MDT track segments are combined with the RPC track if they are consistent in direction and have more than 3 MDT hits. Figure 4 a) shows the resolution of the MDT track segments with respect to the RPC track found by this algorithm. The plot shows the resolution is ≈ 1.8 cm which is consistent with expectations for uncalibrated MDT tubes. Figure 4 b) shows the ϕ distribution of the muon candidates found by the algorithm showing that the muons are coming from above as expected for cosmic rays.

The LAr algorithm searched for the highest energy deposit in the LAr calorimeter and then builds a cluster of size $\Delta\eta = 0.075, \Delta\phi = 0.125$ around this deposit. A plot of the cluster energy is shown in figure 5. This shows a peak at ≈ 0 which comes from calorimeter noise and a shoulder to positive energies which comes from the cosmic ray muon energy deposits (the average energy deposit is ≈ 700 MeV).

3.4. Algorithms run in August cosmic run

In the August run more HLT algorithms were run. The LAr algorithm described above was run but also using information from the Tile calorimeter. A different algorithm (adapted from a physics LVL2 algorithm) which finds muon candidates in the Tile calorimeter was also run.

For the first time a tracking algorithm was run. This LVL2 algorithm uses information from the TRT to find tracks. It has a rather loose cut on the number of TRT hits needed to form a track of 9. Simulation studies show that with number of hits nearly all the found tracks are
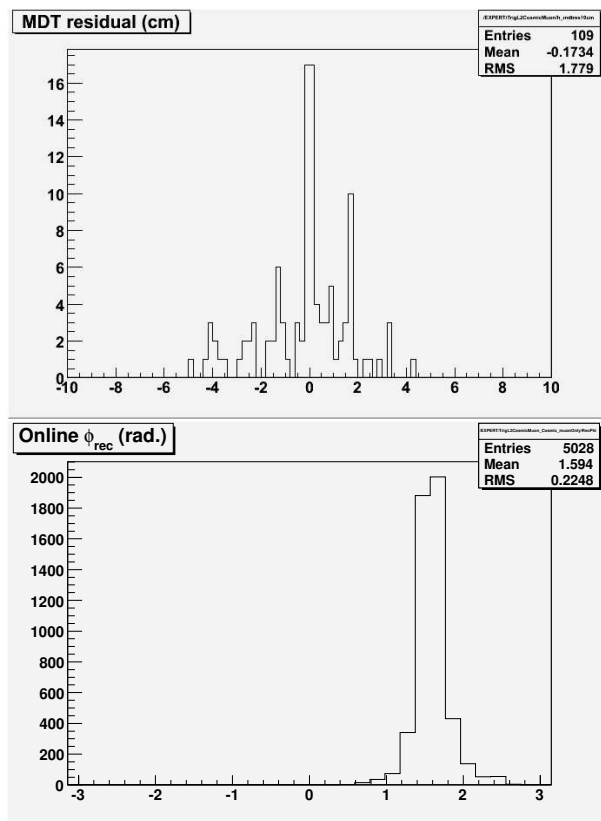
Figure 4. a) (top) The resolution of the MDT track segments with respect to the RPC track found by the LVL2 muon algorithm. b) (bottom) The ϕ of the muon candidates found by the LVL2 muon algorithm.
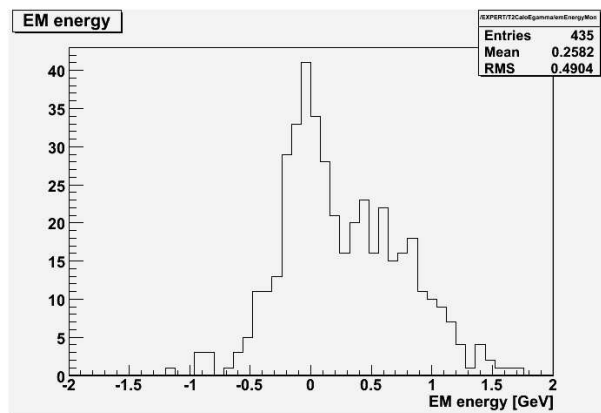
Figure 5. The EM cluster energy from the LVL2 LAr algorithm, running in the June cosmic run. The peak at ≈ 0 GeV is calorimeter noise, whereas the shoulder to positive energies (peaking at ≈ 700 MeV) is the cosmic muon signal. This plot is one of the online histograms produced when the algorithm is running.
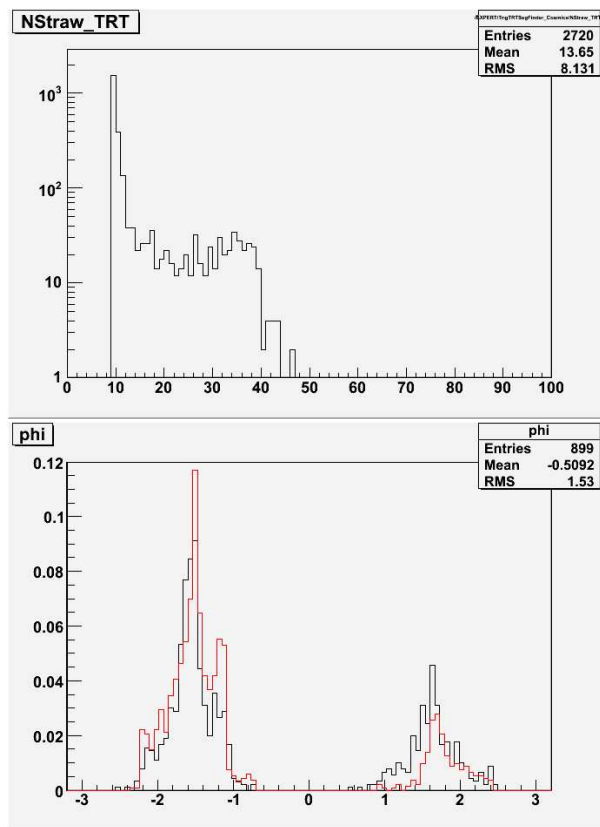
Figure 6. a) (top) The number of TRT hits associated to the tracks found by the TRT LVL2 algorithm running in the August cosmic run. The tracks with <15 hits are dominated by fakes, whereas the tracks with >15 are mostly real tracks. b) (bottom) The ϕ distribution of the TRT tracks found at LVL2. The red shows the real cosmic data from the August cosmic run, whereas the black is simulated data of the same setup (both plots are normalised to unit area).

fakes – however as the number of hits increases above ≈ 15 most of the tracks are real. Figure 6 a) shows the number of hits associated to the tracks found when running online in the August cosmic run. Most of the tracks found are fakes but the bump at number of hits greater than 15 are real tracks.

The ϕ distribution of the tracks found by the algorithm is shown in figure 6 b), where tracks with positive ϕ are in the top half of the detector and tracks with negative ϕ are in the bottom half. The distribution looks as it does due to the available coverage of the TRT. The red plot shows the distribution from real cosmic data taken in the August run whereas the black distribution comes from cosmic simulation for the same TRT setup, the plots are normalised to unit area.

To check that the TRT tracks found are good tracks, a comparison of the track parameters between LVL2 and offline reconstruction has been carried out. Figure 7 shows the comparison of the ϕ and impact parameter ($d0$) of the tracks for events where both LVL2 and offline found a track (LVL2 finds tracks in many more events than the offline tracking as it has a much looser requirement on the number of TRT hits on the track).

During the August cosmic run event filter algorthms were run online for the first time. The algorithms were very simple and just counted hits in the TRT and muon detectors, but these succesfully tested the interface between LVL2 and the event filter.
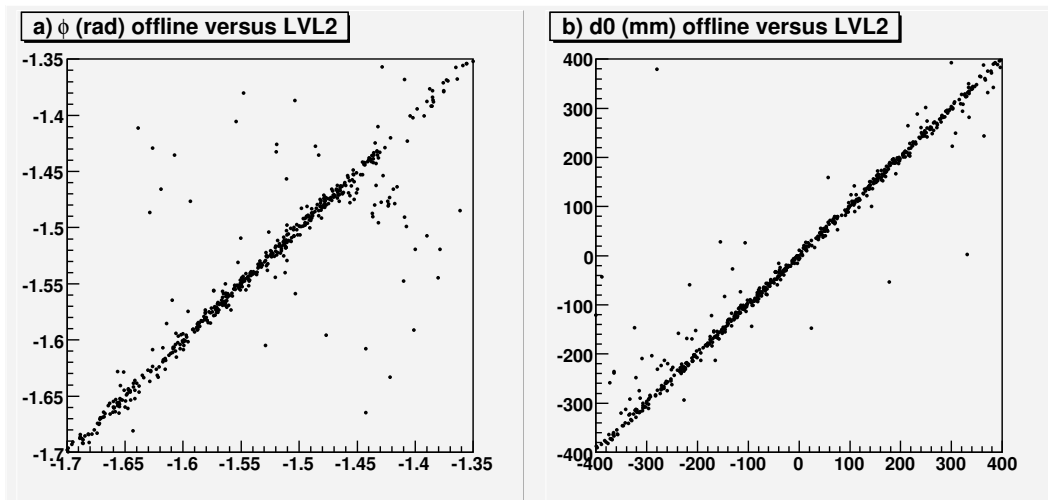
Figure 7. A comparison of the LVL2 (y-axis) and offline tracking (x-axis) track parameters, for events which found an offline and LVL2 track. a) is for the track ϕ, and b) is for the track $d0$.

4. Future use of cosmics

Cosmics rays are not only useful during the commissioning of ATLAS, but also can be very useful during physics running. They can be used for calibrations and for alignment studies (they can be particuarly useful for constraining alignment parameters insensitive to tracks coming from the interaction point). It is therefore important to be able to aquire sufficient samples of cosmic rays during physics running. One possibility is to take cosmic ray runs between physics runs or when the beams are lost, another option being looked into is to take cosmics in the long-gap during physics runs. The long gap is a period of 2.75 μs in each 89 μs orbit ($\approx 3\%$) when there are no protons in the machine. Either way the HLT algorithms used during commissioning (and described in this paper) will play a valuable role in refining the cosmics selected at LVL1.

5. Conclusions

The installation and integration of the ATLAS trigger system is now in full swing. Two combined cosmic ray commissioning runs in summer 2007 have been used to thoroughly test almost the full trigger system. During these runs part of the LVL1 muon barrel and endcap triggers were run using final hardware. For the first time HLT algorithms were run online, with encouraging results. Further combined runs will test the system with greater detector coverage and more HLT algorithms. The current tests show the ATLAS trigger is in excellent shape to be fully functional for collission data taking in summer 2008.

6. Acknowledgements

The commissioning work described in this paper required many things to be working, from the detectors systems through to the offline software. We would like to acknowledge the huge contribution from the whole ATLAS collaboration for their work in getting this working.

7. References

[1] The ATLAS Collaboration, "First-level Trigger Technical Design Report", CERN/LHCC/98-14, 1998.
[2] The ATLAS Collaboration, "High-level Trigger, Data Acquisition and Controls, Technical Design Report", CERN/LHCC/2003-022, 2003.
[3] Stelzer et al, "The Configuration System of the ATLAS Trigger", these proceedings.

[4] George et al, "The ATLAS High Level Trigger Steering" , these proceedings.
[5] Gorini et al, "Integration of the Trigger and Data Acquisition Systems in ATLAS", these proceedings.
[6] Hadavand et al, "Commissioning of the ATLAS offline software with cosmic rays", these proceedings.